https://doi.org/10.20965/jrm.2016.p0600

Development Report:

Upper Body of Dummy Humanoid Robot with Exterior Deformation Mechanism for Evaluation of Assistive Products and Technologies

Kunihiro Ogata*, Tomoya Kawamura, Eiichi Ono*, Tsuyoshi Nakayama*, and Nobuto Matsuhira****

*Research Institute, National Rehabilitation Center for Persons with Disabilities
4-1 Namiki, Tokorozawa City, Saitama 359-8555, Japan
E-mail: {ogata-kunihiro, ono-eiichi, nakayama-tsuyoshi}@rehab.go.jp
**Department of Engineering Science and Mechanics, College of Engineering, Shibaura Institute of Technology
3-7-5 Toyosu, Koto-ku, Tokyo 135-8548, Japan
E-mail: matsuhir@shibaura-it.ac.jp
[Received September 9, 2015; accepted June 1, 2016]

People suffering from tetraplegia are unable to perform many activities of daily living, such as dressing and toileting. The purpose of this study is to develop a dummy humanoid robot to assess assistive products and technologies for patients of tetraplegia. This paper describes the mechanism, motion planning, and sensing system of the dummy robot. The proposed dummy robot has upper-arm mechanisms that simulate the human collarbones based on a functional anatomy. To realize a variety of body shapes, the proposed robot has deformation mechanisms that use linear actuators and rotating servo-motors. The sensing system of the dummy robot can measure clothing pressure before and after exterior deformation is measured, and can hence detect changes in it.

Keywords: humanoid robots, dummy robots, spinal cord injury, dressing

1. Introduction

Spinal cord damage can significantly curtail a person's mobility and other body functions, and can lead to muscle weakness and paralysis. Many people with tetraplegia have great difficulty in living independent lives, are limited in their activities of daily living (ADL), and typically require the use of a manual or electric-powered wheelchair to move. When the independence rates of patients of tetraplegia (complete lesions at level C4 to T1), which were rated on a four-point scale, were calculated, the rates for "eating" and "bed, wheelchair transfer" were found to be high; on the contrary, the rates for "dressing" and "toileting" were low [1]. Moreover, the increased time spent "toileting" and "dressing" by people with tetraplegia may be a reflection of their lower residual function causing balance and coordination tasks to take longer to complete [2].

Patients with spinal cord injuries typically use wheelchairs and sit in the same position for lengthy periods. Moreover, elderly patients may have a limited range of movement and may spend a significant amount of time seated. Therefore, they are at risk of developing pressure ulcers, which are injuries to the skin and the underlying tissue resulting from prolonged pressure on the skin [a]. To prevent pressure ulcers, the body of the patient is turned or depressurized at regular intervals. Pressure ulcers most often develop on skin covering bony areas of the body, such as the ischial bone and tailbone [3]. Therefore, seats and cushions for wheelchairs must help reduce pressure on the skin. Some people with tetraplegia take a long time to defecate, hence spend a lengthy period seated on the toilet seat, and thus suffer the risk of developing pressure ulcers. Therefore, clothes and toilet sheets should be designed to help those with spinal cord injuries live independently.

In general, attire is expected to be functional as well as fashionable. The European research project "Fashionable" involved the development of integrated technologies to meet the requirements of people with physical disabilities and special needs [b]. The National Rehabilitation Center for Persons with Disabilities held a fashion show – the *KOKURIHA* fashion show – to arouse people's interest in fashionable and functional clothing. Fashionable and functional clothes are expected to promote social participation of persons with disabilities.

To promote the development of clothes and toilet seats for people with a spinal cord injuries, such equipment needs to be tested. Therefore, the purpose of this study is to develop a device to test such assistive products and technologies.

2. Dummy Humanoid Robot with Exterior Deformation Mechanism

To evaluate clothing and assistive products and technologies, a device that can simulate the human body is proposed here.

2.1. Past Dummy Research

Several robots to simulate the human body have been developed in the past. Dummy robots to simulate a patient have also been developed and used for medical education. Ishii et al. developed a humanoid robot for airway management training [4]. This robot was equipped with force sensors that were used to score the airway management performance of trainees in order for them to subsequently be able to observe their efforts. Showa University and TMSUK developed a dental patient robot called "Hanako2 Showa" [c]. This robot looks like a woman, and has been programmed with certain behaviors used to objectively evaluate the clinical ability of medical students. A method to test a power-assistant device using the humanoid robot HRP-4C has also been proposed [5]. The humanoid robot wears a "Smart Suit Lite" and measures the joint torque of the body. Several human body parameters that are difficult to estimate directly can be obtained using robotics techniques. The shape of HRP-4C is similar to that of an average Japanese female and, therefore, the shape of the robot has to deform to treat various human bodies. Some robots have been designed to focus on the shape of the human body. To act as substitutes for real people trying on clothes, robotic mannequins were developed. Theses robots can change their shapes and imitate different human body types [6]. The mechanism of deformation is necessary to assess the suitability of attire or wearable devices for persons. This robotic mannequin did not have four limbs, and maintained a standing posture.

Therefore, a dummy robot with both a multi-linked body mechanism and a deformation mechanism is proposed in this study.

2.2. Humanoid Robot Simulating Person with Spinal Cord Injury

The motor functions of a patient with a spinal cord injury differ depending on the area of the nerve injury [7]. Patients with a C5 spinal cord injury have difficulty in straightening their elbow joints, whereas patients with a C7 injury can straighten their elbows. Some patients with a cervical cord injury (over C8) have disabilities in their upper limbs because of weakened upper limb muscles, moreover, some patients with a spinal cord injury (below T1) have sufficient motor function in their upper limbs to roll a wheelchair by themselves, with their upper-arm muscles having been developed, as well as a widespread joint range of the upper limbs to independently carry out many ADLs. The physical activity level (PAL) of persons with paraplegia is lower than that of able-bodied adults, and most participants are obese [8]. The body shapes of persons with spinal cord injuries may be statistically different from those of able-bodied adults. Considering the reduced and increased muscle mass and the accumulation of abdominal fat, it is necessary to extend the exterior of the shoulder, chest, arm and abdomen as the maximum deformation between 30 mm and 90 mm.

Therefore, the proposed dummy robot should have a deformation mechanism of the shoulders and stomach to adapt to several levels of spinal cord damage. The proposed dummy robot must have an upper-limb mechanism based on the human body to realize several daily motions, such as wheeling motion and reaching motions.

In this study, in order to measure the contact force from the environment, tactile sensors should be implemented throughout the body of the dummy robot. In particular, the dummy robot should be expected to clarify the wear comfort or easy-to-wear nature of clothing based on clothing pressure.

This paper describes the development of the proposed dummy robot, and a system for evaluating clothing with respect to the body shape of persons with a spinal cord injury.

3. Mechanism of Superior Limb Girdle

This section is dedicated to a description of the mechanism of a superior limb girdle. The joint range of the superior limb of the proposed dummy robot needs to be wide. Thus, a superior limb mechanism with a collarbone link is proposed in this paper.

The superior limb of a human consists of a collarbone, blade bone, upper-arm bone, ulna, and radius. However, most humanoid robots only have a mechanism simulating the upper-arm and forearm, the motion range of which is narrow. Therefore, several robots with a mechanism simulating the collarbone and blade bone have been developed. Ikemoto et al. developed a superior limb girdle robot driven by McKibben pneumatic artificial muscles. This robot realized dynamic throwing motions [9].

To realize real human motions using humanoid robots with a wide joint range, a mechanism is needed to simulate the motions of the collarbone [10]. This study is aimed at developing a superior limb mechanism that realizes various poses as well as a deformation of body shape. Moreover, the function of this dummy robot is sufficient to realize several static poses, but dynamic motion is not treated.

3.1. Robot Arms with Collarbone Link

The degree of freedom (DOF) of a human superior limb girdle includes flexion motion along the horizontal plane and abduction motion along the lateral plane [10]. Thus, the arm of the proposed robot has two DOFs to control the position of the shoulder, three DOFs to control the altitude of the upper-arm, and an elbow joint (with one DOF). This robot arm does not have any DOF for the wrist because the hand contributes little to the mobility of the wearer.

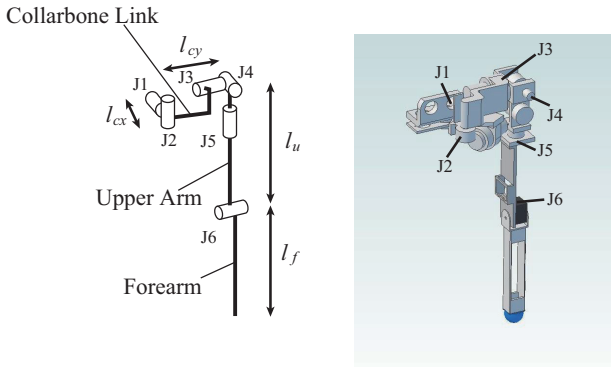

(a) Link Model (b) 3D CAD data

Fig. 1. Mechanism of robot arm with a collarbone link.

Table 1. The specifications of the range of motion and the actuator of each joint.

	Joint motion range [°]	Desired max. torque [Nm]	Actual max. torque [Nm]
J1	25	7.90	12.1
J2	40	7.17	9.49
J3	230	2.90	3.16
J4	90	2.90	4.74
J5	130	5.67	4.09
J6	120	4.08	4.09

The outline of this robotic mechanism is shown in **Fig. 1**, and the range of motion of each joint is determined based on [10] as shown in **Table 1**.

The desired maximum torque of each joint within the joint motion range is calculated and listed in **Table 1**.

This mechanism uses harmonic drives and bevel gears. The drive mechanisms can be set in small areas, and there is sufficient space at the chest and shoulders to implement a deformation mechanism to realize various body shapes. The actual maximum joint torque is shown in **Table 1**. This superior limb girdle mechanism is considered for use in the deformation mechanism. This dummy robot can realize various poses and body shapes, and can simultaneously measure the pressure on the surface of the robot (i.e., the clothing pressures). Thus, various types of clothing can be tested.

3.2. Motion Range of the Proposed Robot Arms

The working areas of the arms of proposed dummy robot on the sagittal plane, the lateral plane, and the horizontal plane were calculated under conditions where the motion of the collarbone-link was both constrained and unconstrained. These working areas were then compared, and the increase in the rate of the working areas was calculated. The extension and the flexion of the shoulder along the sagittal plane (z-x plane), the abduction and adduction of the shoulder along the lateral plane (y-z plane), and the extension and the flexion of the shoulder along the horizontal plane (x-y plane) were calculated. The results are listed in **Table 2**.

Table 2. Calculation results of the reachable region of the robotic arm.

	Without collarbone link [m^2]	With collarbone link [m^2]	Rate of increase [%]
x-y plane	0.23	0.36	57
y-z plane	0.34	0.43	28
z-x plane	0.44	0.70	60

The calculation results show that the working area along the sagittal plane increased by 60%, that along the lateral plane increased by 28%, and the working area along the horizontal plane increased by 57%. Therefore, the increase in the working areas of the dummy robot with a collarbone-link was confirmed.

3.3. Singular Posture

The joint angles were calculated though inverse kinematics based on the position of the hand and the altitude of the upper limb. When the joint angles of singular postures were calculated using an inverse kinematics algorithm, the solution of the joint angles was underspecified, and the computation algorithm indicated instability. The singular postures of the dummy robot were then considered. The determinant of the Jacobian matrix J of the upper limb mechanism is shown in Eq. (1), and each parameter of the Jacobian matrix is shown in **Fig. 1**.

$$\begin{aligned} det\,(J) = & -l_u \cos\theta_4 \,(l_{cy}\cos\theta_2 + l_{cx}\sin\theta_2) \\ & (l_{cx}\cos\theta_3\cos\theta_5 + l_{cy}\cos\theta_4\sin\theta_5 \\ & + l_{cx}\sin\theta_3\sin\theta_4\sin\theta_5) \quad \ldots\ldots \quad (1) \end{aligned}$$

From Eq. (1), the determinant of the Jacobian matrix was zero with respect to several patterns of each joint angle, such as $\theta_4 = \pi/2$. The motions of the upper limb were then calculated using inverse kinematics algorithms that could steadily compute around singular postures [11].

3.4. Simulations of Superior Limb Motion

The proposed dummy robot was developed to test clothing, and assistive products and technologies, and therefore must be able to facilitate the activities of daily life of wheel-chair users. In this study, wheeling motion was calculated using an inverse kinematics algorithm. As described in Section 3.3, the robot arm had several singular poses, and the motions of the robotic arm were calculated using the Levenberg-Marquardt method [11]. This method can be used to stably and quickly calculate inverse kinematics.

The trajectory of the wheeling motion was calculated

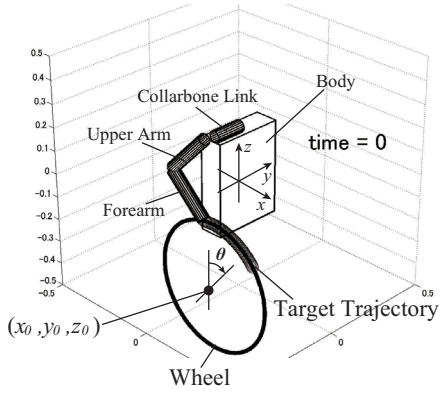

Fig. 2. Simulation environment showing the coordinate origin, robot arm, wheel and target trajectory.

Table 3. Each parameter of the simulation of the motion of the superior limb.

	[m]		[m]
l_{cx}	0.04	x_0	0.05
l_{cy}	0.179	y_0	−0.19
l_u	0.266	z_0	−0.405
l_f	0.240	r	0.28

using the following set of equations:

$$\begin{cases} x_{ref} = x_0 + r\sin(\theta) \\ y_{ref} = y_0 \\ z_{ref} = z_0 + r\cos(\theta) \end{cases} \quad \ldots\ldots\ldots \quad (2)$$

where, $[x_{ref}, y_{ref}, z_{ref}]^T$ is the target position of the hand, and $[x_0, y_0, z_0]^T$, r, and θ are the center, radius, and exterior angle of the wheel, respectively (see **Fig. 2**). The value of the simulation parameters is shown in **Table 3**.

The calculation results involving motions of the collarbone link were compared with calculation results where joints J1 and J2 were fixed to zero. A snapshot of the simulation is shown in **Fig. 3**, the calculated joint angles are shown in **Fig. 4**, and the hand trajectories are shown in **Fig. 5**.

From **Fig. 5**, each calculation result tracked the target value; however, there was a difference in the angle trajectories between the two calculation results. The calculation results of J1, J2, J4, and J5 with the collarbone link changed significantly, but the results of J3 (shoulder pitch) and J6 (elbow) change only slightly, comparison with the results obtained without a collarbone link. Based on these results, motion compensating those of the shoulder and elbow along the pitch axis was generated by the proposed superior limb mechanism.

When the dummy robot was tested for clothing and the assistive products and technologies, the wheeling motion was calculated based on the body movements of wheelchair users. The measurement and analysis of the ADL of wheelchair users will form the focus of future research in the area.

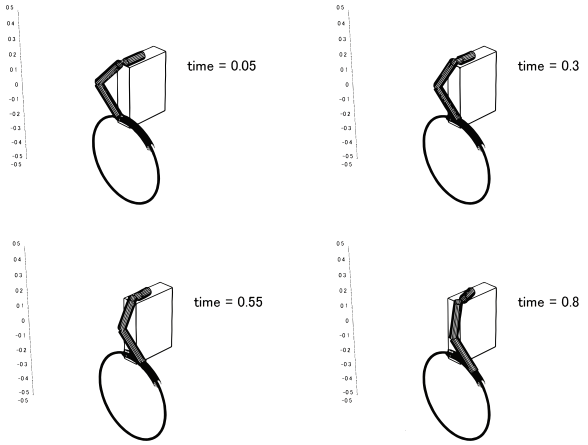

(a) Robot arm with a collarbone link

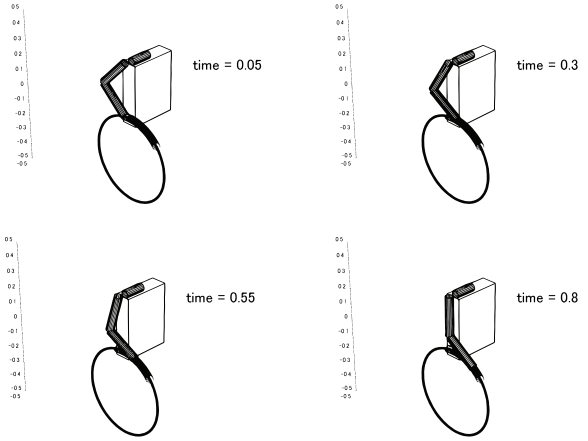

(b) Robot arm without a collarbone link

Fig. 3. Snapshots of each simulation condition. (a) The motion was calculated using inverse kinematics involving the collarbone link. (b) Motion was calculated without the collarbone link.

4. Mechanism of Exterior Deformation

The bodies of patients with damaged spinal cords are different from those of healthy people according to the level of spinal cord injury and lifestyle. The dummy robot needs to change its body shape in order to test different types of clothing. Some people with damaged spinal cords can translate their bodies using their upper limbs, which they can use to roll wheelchairs themselves because the circumference of their upper arms, and the thickness of their chests and shoulder muscles tend to be greater than those of healthy people. At the same time, the amount of abdominal subcutaneous fat is higher in them, and the circumference of their abdomen may be greater as well.

4.1. Deformation Mechanism of the Arm and Body

The dummy robot has joints in the pectoral girdle to adjust the pose of the upper limbs. Therefore, the deformation mechanism was mounted to allow the dummy robot to assume several poses. The degree of the deformation was decided based on the difference between the

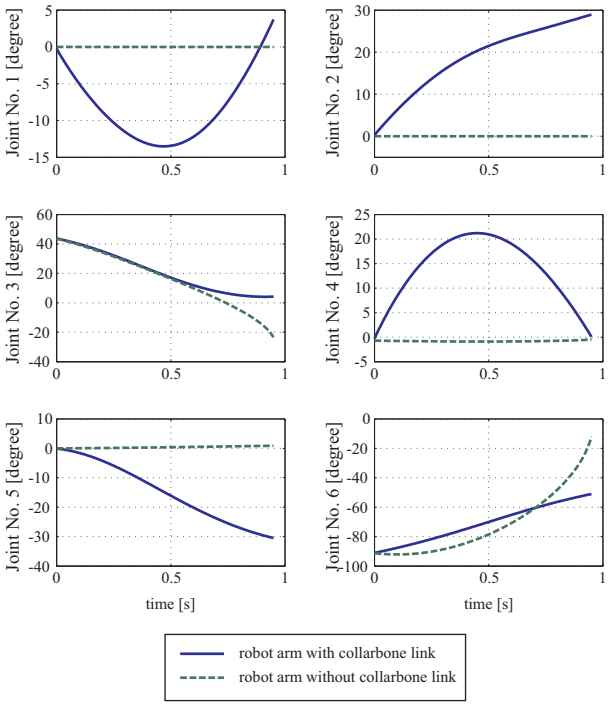

Fig. 4. Simulation results of joint angles calculated through the inverse kinematics.

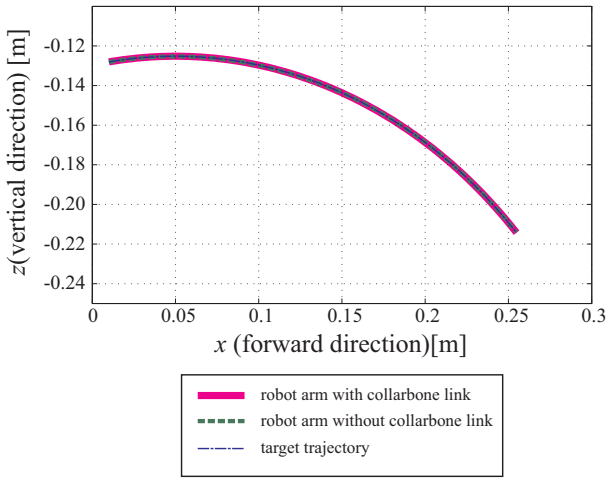

Fig. 5. Hand trajectories determined by joint angles calculated by inverse kinematics and target trajectories.

average and the maximum calculated by [d], in consideration of the space in the trunk of the robot. The trunk of the dummy had linear actuators to realize expanding deformation. The deformation mechanism with linear actuators is shown in **Fig. 6**, which shows Miniature Linear Actuators developed by Firgelli Technologies, Inc., with strokes/maximum lengths of 30 and 50 mm. The dummy robot controlled these linear actuators to adjust its body shape.

Moreover, the linear actuators could not be mounted on the superior limb girdle mechanism, and the deformation of the superior limb was instead realized by rotating the servo-motors. The deformation mechanism using the rotation motors is shown in **Fig. 7**.

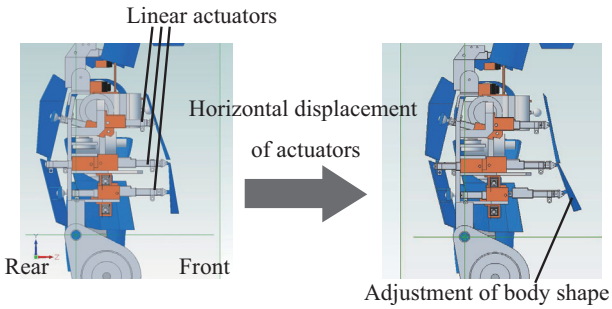

Fig. 6. Exterior deformation mechanism of chest region using linear actuators.

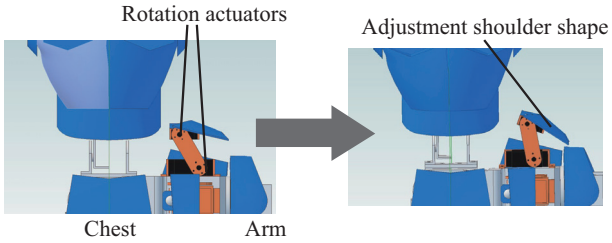

Fig. 7. Exterior deformation mechanism of shoulder using rotating servo motors.

4.2. Tactile Sensor

Some robots that use tactile sensors on their entire bodies have been developed to communicate with humans and generate several types of motion. Ohmura et al. developed tactile sensors and implemented these on a humanoid robot to achieve whole-body motion with tactile feedback control [12, 13]. Maggiali et al. developed an artificial skin system based on a conformable mesh of sensors in a triangular shape. These sensors were interconnected to form a networked structure [14]. They simulated the human skin to monitor the pressure on the entire body. "Macra" can monitor the deformation of the soft structure of the entire body using three-axis force sensors, and can sense several contact states using human communication [15]. However, this sensing system provides only coarse resolution, and more expensive sensors are needed for higher-quality resolution.

The sensing mechanism of the dummy robot was developed based on the mechanism of the sensor in reference [12]. This photo-reflective sensor consisted of a light-emitting diode (LED) and a photo-detector. The scattering ray generated from the LED changed through the deformation of the urethane foam, and this change was measured by a photo-detector. The sensing mechanism is shown in **Figs. 8(a)** and **(b)**.

The sensor was evaluated by adding test weights (1 g, 2 g, 5 g, 10 g, 20 g, 50 g, and 100 g) to it. As value of pressure, the load of each test weight divided by the area of each test weight was used. The area of each test weight was calculated based on the size and shape of each test weight. The measurement results are shown in **Fig. 9(a)**. The horizontal axis indicates the sensor value (voltage),

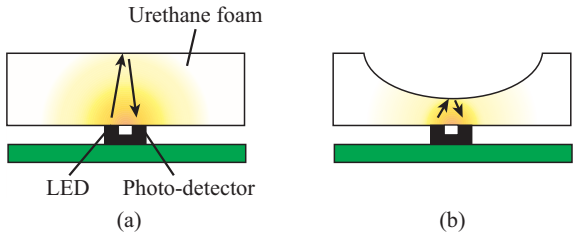

Fig. 8. Mechanism of the tactile sensors: (a) before and (b) after pressurizing the urethane foam.

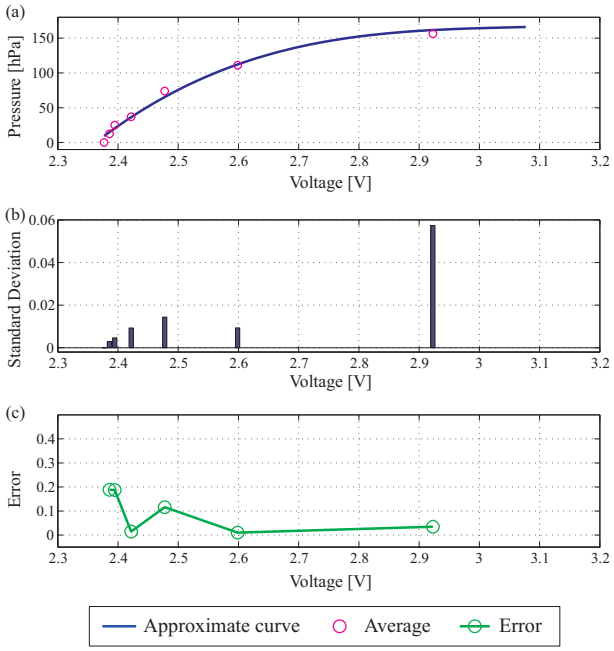

Fig. 9. Measurement results of the tactile sensor, and the approximate curve calculated using multiple regression analysis.

and the vertical axis shows the pressure value. Reference [16] has shown that comfortable pressure values for clothing range from 19.6 hPa to 39.2 hPa, and uncomfortable ones from 58.8 hPa to 98.0 hPa. Thus, these ranges of clothing pressure were included in the measurement range of the sensor in our study.

From **Fig. 9(a)**, it is clear that the sensor obtained values in comfortable and uncomfortable pressure ranges. Moreover, the non-linear curve of pressure values can be estimated based on the voltage using a regression algorithm. The cubic polynomial computed using a multiple linear regression analysis of voltage and pressure based on the results of **Fig. 9(a)** is thus shown in Eq. (3), and the standard deviation of the sensor value is shown in **Fig. 9(b)**.

$$p = 448.01v^3 - 4110.3v^2 + 12592v - 12714 \quad . \quad (3)$$

where, p [hPa] is the pressure on the sensor, and v [V] is its voltage. Using this approximate curve, the value of the pressure applied to sensors can be estimated based on the sensor voltage. To calculate the approximate curve, errors

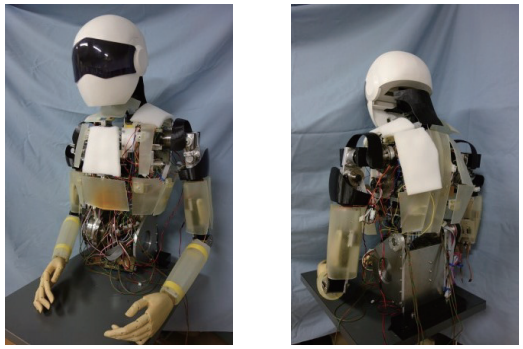

(a) Appearance of Dummy Robot

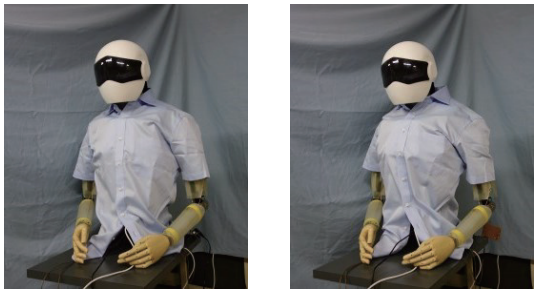

(b) Before Deformation (c) After Deformation

Fig. 10. Appearance of dummy robot. (b) and (c) show the dummy robot wearing a shirt.

between the actual measured values and the those calculated by the approximate curve are shown in **Fig. 9(c)**. The difference between the measured and the estimated values is divided by the measured values, and these normalized values are the errors. The errors were less than 0.20, which is quite small. Therefore, the sensor can evaluate whether clothes are comfortable. The hysteresis of this sensor was not measured in this study; however, the characteristic of the hysteresis may approximate the tactile sensor developed by Ohmura et al. [12].

5. Measuring Clothing Pressure with Exterior Deformation

The clothing pressure on the developed dummy robot system before and after deformation was measured to confirm whether the robot can test the comfort of the worn clothing.

The proposed dummy robot is shown in **Fig. 10(a)**. Each body measurement of the dummy robot was made based on the average anthropometrical data of a Japanese male [d]. The shape of the exterior of the deformation was designed based on a male mannequin on the market. Moreover, the dummy robot wearing a shirt before and after the deformation of its exterior is shown in **Figs. 10(b)** and **(c)**, where the deforming exterior covers the chest, shoulders, and the blade bones.

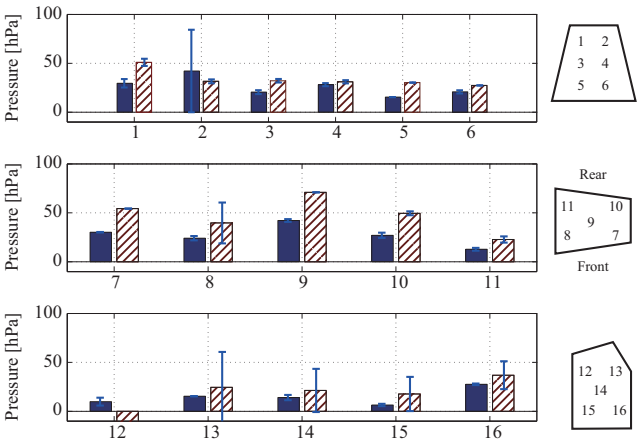

Fig. 11. Experimental results from the tactile sensors before and after exterior deformation.

5.1. Measurement Result

From **Figs. 10(b)** and **(c)**, the chest and shoulders of the dummy robot are expanded by the deformation of the exterior. The linear actuator of the central chest extended by 20 mm. The servo-motors of the left and right chest, shoulder, and blade bones were rotated 20°. Then, the left and right chest, shoulder, and blade were extended to 15 mm. The changes in the tactile sensors are shown in **Fig. 11**, where the relative values of each sensor element were calculated with reference to sensor values without clothing. The solid lines represent sensor values before deformation, and the hatched lines show those after deformation. The numbers along the horizontal axis represent the number of each sensor element along the exterior, where the positions of each sensor are shown on right in **Fig. 11**. Thirty samples were obtained for the steady state of each sensor element, and the average values of each sensor element were calculated. The pressure values were then calculated based on the voltage values using the cubic polynomial in Eq. (3).

Several sensor values (solid lines) were increased through the wearing of clothes, and several tactile sensor values (hatched lines) were increased due to exterior deformation. The second sensor element decreased in value after deformation; however, the variance of the sensor values before deformation was large, and this sensor value before deformation may have been unstable. The variance in the values of the tactile sensor elements along the shoulder (7th, 9th, 10th, and 11th) was smaller than the increasing values of these sensor elements before and after deformation, and these sensor values may have been significantly increased by exterior deformation. The changes in the sensor values along the shoulder were frequent, which means that the clothes may have bound the superior limbs of the person with a spinal cord injury, thereby suggesting that the dummy robot can evaluate the mobility of the clothing.

5.2. Discussion

Tanaka et al. measured the clothing pressure of the entire female human body using Finite Element Method (FEM) simulation [17]. From the simulation results, clothing pressure distributions along the breast and shoulder were the highest for the entire body. The shape of the body was designed based on the female anatomy, and the clothing pressure on the breasts tended to increase. On the contrary, the shape of the dummy robot in this study was developed based on the male human body, and the dummy robot hence did not have a swell in the breasts. Therefore, the clothing pressure along the shoulder was higher than that on the chest.

The measured clothing pressure values before deformation were smaller than 50 hPa, and several values were included in the comfortable pressure range [16]. Then, after the exterior was transformed by deformation, the clothing pressure of the 9th element was found to lie in the uncomfortable ranges, and several clothing pressure values (e.g., 1st, 7th, and 10th) being at around 50 hPa, were also not in the comfortable range. Thus, this shirt did not fit the deformed dummy robot.

In these experiments, the clothing pressure on the blade bone was smaller than on other areas on average. From [18], when male humans lift their upper limbs to 90°, the clothing pressure values of the scapular and back armhole increase. Thus, the clothing pressure may drastically change due to motions of the upper limbs. In future work, the clothing pressure due to various human poses will be measured, and the method of mobility of clothing based on the pattern information concerning the integrated sensor values will be discussed.

This study confirmed a change in the clothing pressure in the static pose of a dummy robot through deformation, thus, confirming the potential of this dummy robot system to simulate the static pose of a person with spinal cord injury. In future research, clothing pressure will be measured when the dummy robot performs the motion of rolling a wheelchair in order to implement a simulation that can capture a unique characteristics of a person with a spinal cord injury.

6. Conclusion

The purpose of this study was to develop a humanoid dummy robot capable of evaluating assistive products and technologies for tetraplegia patients. The proposed dummy robot simulates a person with a spinal cord injury, has a large movable range in its upper limbs, and is incorporated with a mechanism for changing its body shape. Tactile sensing systems were developed to measure the clothing pressure on the dummy robot. These sensors were then implemented on the exterior of the dummy robot, and confirmed the increase in clothing pressure based on exterior deformation.

In future research, several daily movements of a person with spinal cord injury will be measured and imple-

mented on the dummy robot in order to establish even more sophisticated criteria for clothes using tactile sensors based on actual data of spinal cord injury. Moreover, the lower body of the dummy robot will be developed to evaluate the risk of pressure ulcers. The criteria for evaluating the clothing and toilet seat for a person with a spinal cord injury were established using the proposed humanoid dummy robot.

Acknowledgements

This work was supported by JSPS KAKENHI Grant Number 25282181.

References:

[1] J. Jongjit, W. Sutharom, L. Komsopapong, N. Numpechitra, and P. Songjakkaew, "Functional Independence and Rehabilitation Outcome in Traumatic Spinal Cord Injury," The Southeast Asian J. of Tropical Medicine and Public Health, Vol.35, No.4, pp. 980-985, 2004.

[2] S. P. Hetz, A. E. Latimer, and K. A. Martin Ginis, "Activities of daily living performed by individuals with SCI: Relationships with physical fitness and leisure time physical activity," Spinal Cord, Vol.47, No.7, pp. 550-554, 2009.

[3] D. J. Gosnell, "Assessment and evaluation of pressure sores," Nurs. Clin. North. Am, Vol.22, No.2, pp. 399-416, 1987.

[4] H. Ishii and A. Takanishi, "Robotic patient simulator for medical skills training," Trans. of Japanese Society for Medical and Biological Engineering, Vol.51, p. M-105, 2013.

[5] Y. Imamura, T. Tanaka, K. Ayusawa, and E. Yoshida, "Verification of Assistive Effect Generated by Passive Power-Assist Device Using Humanoid Robot," Proc. of the 2014 IEEE/SICE Int. Symposium on System Integration, pp. 761-766, 2014.

[6] A. Abels and M. Kruusmaa, "Construction of a Female Shape-Changing Robotic Mannequin," J. of Automation and Control Engineering, Vol.1, No.2, pp. 132-134, 2013.

[7] F. M. Maynard, M. B. Bracken, G. Creasey, J. F. Ditunno, W. H. Donovan, T. B. Ducker, S. L. Garber, R. J. Marino, S. L. Stover, C. H. Tator, R. L. Waters, J. E. Wilberger, and W. Young, "International Standards for Neurological and Functional Classification of Spinal Cord Injury," Spinal Cord, Vol.35, No.5, pp. 266-274, 1997.

[8] A. C. Buchholz, C. F. McGillivray, and P. B. Pencharz, "Physical Activity Levels Are Low in Free-Living Adults with Chronic Paraplegia," Obesity Research, Vol.11, No.4, pp. 563-570, 2003.

[9] S. Ikemoto, F. Kannou, and K. Hosoda, "Humanlike shoulder complex for musculoskeletal robot arms," 2012 IEEE/RSJ Int. Conf. on Intelligent Robots and Systems (IROS), pp. 4892-4897, 2012.

[10] I. A. Kapandji, "Anatomie Fonctiionnelle Tome 1, Membre superieur, 6e ed," MALOINE, 2005 (in French).
ISBN: 9782224026479.

[11] T. Sugihara, "Solvability-unconcerned Inverse Kinematics based on Levenberg-Marquardt Method," 2009 IEEE-RAS Int. Conf. on Humanoid Robots, pp. 555-560, Paris, Dec. 9th, 2009.

[12] Y. Ohmura, Y. Kuniyoshi, and A. Nagakubo, "Conformable and Scalable Tactile Sensor Skin for Curved Surfaces," Proc. IEEE Int. Conf. on Robotics and Automation, pp. 1348-1353, 2006.

[13] Y. Ohmura and Y. Kuniyoshi, "Humanoid robot which can lift a 30kg box by whole body contact and tactile feedback," IEEE/RSJ Int. Conf. on Intelligent Robots and Systems 2007 (IROS 2007), pp. 1136-1141, 2007.

[14] M. Maggiali, G. Cannata, P. Maiolino, G. Metta, M. Randazzo, and G. Sandini, "Embedded Distributed Capacitive Tactile Sensor," Mechatronics 2008, pp. 1-5, 2008.

[15] M. Hayashi, T. Yoshikai, and M. Inaba, "Development of a Humanoid with Dis-tributed Multi-Axis Deformation Sense with Full-Body Soft Plastic Foam Cover as Flesh of a Robot," InTech, 2008. DOI: 10.5772/6629.

[16] H.-Y. Li, "Research on relationship between materials and internal function design of clothing," Int. Conf. on Fibrous Materials 2009, pp. 1089-1092, 2009.

[17] M .Tanaka, H. Noguchi, M. Fujikawa, M. Sato, S. Oi, T. Kobayashi, K. Furuichi, S. Ishimaru, and C. Nonomura, "Development of Large Strain Shell Elements for Woven Fabrics with Application to Clothing Pressure Distribution Problem," Computer Modelling in Engineering and Sciences, Vol.62, No.3, pp. 265-290, 2010.

[18] D. Chen and Y. Gan, "A Study on Clothing Pressure of the Men's Suit for Comfort Evaluation – Relationship between Clothing Pressure and Clothing Comfort –, " Clothing Research J., Vol.2, No.1, pp. 61-66, 2004.

Supporting Online Materials:

[a] National Pressure Ulcer Advisory Panel: Pressure Ulcer Prevention Points IV, Mechanical Loading and Support Surfaces.
http://www.npuap.org/wp-content/uploads/2012/03/PU_Prev_Points.pdf [Accessed September 9, 2015]

[b] European Research Project Fashionable.
http://www.fashionable-project.eu/ [Accessed September 9, 2015]

[c] "Official curriculum for dentistry by robot, first in the world. More humanized Showa Hanako 2debut," 2011.
http://www.tmsuk.co.jp/topic/2011/06/detail15.html
[Accessed September 9, 2015]

[d] AIST Digital Human Research Center.
http://www.dh.aist.go.jp/en/ [Accessed September 9, 2015]

Name:
Kunihiro Ogata

Affiliation:
Researcher, Service Robotics Research Team, Robot Innovation Research Center, National Institute of Advanced Industrial Science and Technology (AIST)

Address:
1-1-1 Umezono, Tsukuba, Ibaraki 305-8568, Japan

Brief Biographical History:
2012- National Rehabilitation Center for Persons with Disabilities
2014- Saitama University
2016- National Institute of Advanced Industrial Science and Technology (AIST)

Main Works:
• "Training Assist System of a Lower Limb Prosthetic Visualizing Floor-Reaction Forces Using a Color-Depth Sensing Camera," IEICE Trans. on Information and Systems, Vol.E98-D, No.11 pp. 1916-1922, 2015.

Membership in Academic Societies:
• The Robotics Society of Japan (RSJ)
• The Institute of Electronics, Information and Communication Engineers (IEICE)
• The Institute of Electrical and Electronic Engineers (IEEE)

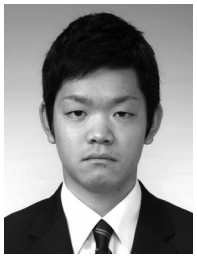

Name:
Tomoya Kawamura

Affiliation:
Shibaura Institute of Technology

Address:
3-7-5 Toyosu, Koto-ku, Tokyo 135-8548, Japan

Brief Biographical History:
2010- Department of Engineering Science and Mechanics, Shibaura Institute of Technology
2014- Graduate School of Engineering and Science, Shibaura Institute of Technology

Main Works:
• "Mechanical Design and Motion Planning of the Robot Arm for Clothes Evaluation of Wheelchair Users," SI2014, 3D1-2, pp. 1999-2003, 2014 (in Japanese).

Name:
Eiichi Ono

Affiliation:
Director, Research Institute, National Rehabilitation Center for Persons with Disabilities

Address:
4-1 Namiki, Tokorozawa, Saitama 359-8555, Japan

Brief Biographical History:
1983-1992 Research Institute for Polymers and Textiles
1994-2000 Electrotechnical Laboratory
2010- Research Institute, National Rehabilitation Center for Persons with Disabilities

Main Works:
• "Fiber for Rehabilitation Uplifts Your Fashion and Invigorates," Sen'i Gakkaishi, Vol.69, No.11, Nov. 2013.
• "Expectation for Robotics (Style of Care and QOL of Patients)," Rehabilitation Nursing, Shin-taikei, Kangogaku-zensho, Bekkann, Medical-friend Co., pp. 393-400, Jan. 2015.

Membership in Academic Societies:
• The Japan Society of Mechanical Engineers (JSME)
• The Robotics Society of Japan (RSJ)
• Rehabilitation Engendering Society of Japan (RESJA)

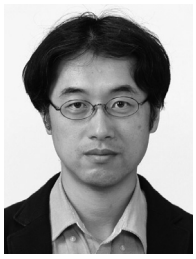

Name:
Tsuyoshi Nakayama

Affiliation:
Section Chief, Principal Investigator, Research Institute, National Rehabilitation Center for Persons with Disabilities

Address:
4-1 Namiki, Tokorozawa, Saitama 359-8555, Japan

Brief Biographical History:
1996- Joined National Rehabilitation Center for Persons with Disabilities

Main Works:
• T. Nakayama et al., "Mobile Phone Application for Supporting Persons with Higher Brain Dysfunctions," IEEJ Trans. on Electronics, Information and Systems, Vol.130, No.3, pp. 394-400, 2010.
• I. Yoda, K. Itoh, and T. Nakayama, "Collection and Classification of Gestures from People with Severe Motor Dysfunction for Developing Modular Gesture Interface," HCI Int. 2015, Los Angeles, USA, August 2-7, 2015, Springer International Publishing Switzerland 2015, UAHCI, Part II, LNCS Vol.9176, pp. 58-68, 2015.
• T. Kinoshita, T. Nakayama et al., "Usability of assistive robotic arms for individuals with severe physical disabilities," 16th Int. Congress of the World Federation of Occupational Therapists in collaboration with the 48th Japanese Occupational Therapy Congress and Expo, CI1-2-4, Yokohama, June 18-21, 2014.

Membership in Academic Societies:
• The Japanese Society for Wellbeing Science and Assistive Technology
• The Society of Life Support Engineering
• The Institute of Electronics, Information and Communication Engineers (IEICE)

Name:
Nobuto Matsuhira

Affiliation:
Professor, Department of Engineering Science and Mechanics, Shibaura Institute of Technology

Address:
3-7-5 Toyosu, Koto-ku, Tokyo 135-8548, Japan

Brief Biographical History:
1982- Toshiba Corp.
2004-2007 Visiting Professor, Tokyo Institute of Technology
2016- Shibaura Institute of Technology

Main Works:
• "Research and Development for Life Support Robots that Coexist in Harmony with People," Mobile Robots, Advanced Robotic Systems International, pp. 287-308, 2006.

Membership in Academic Societies:
• The Japan Society of Mechanical Engineers (JSME)
• The Robotics Society of Japan (RSJ)
• The Institute of Electrical and Electronics Engineers (IEEE) Robotics and Automation Society